Supporting information

Supporting Figure 1

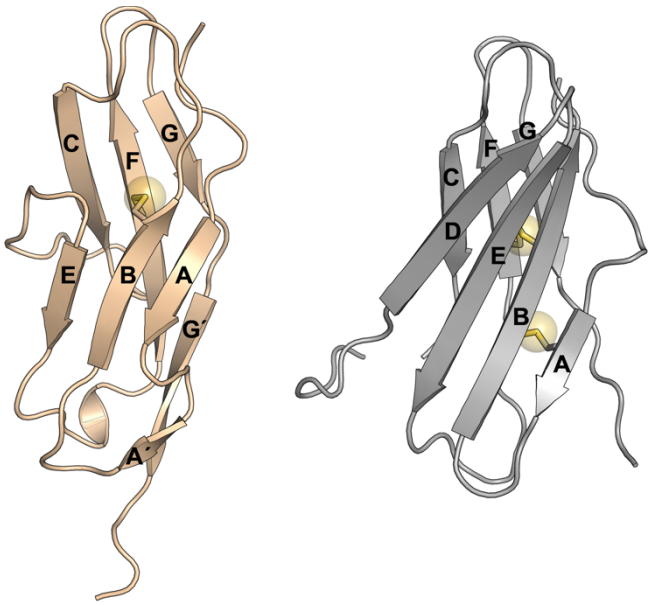

C2-type Ig domain
$CD22_{d7}$

C1-type Ig domain
MAG_{d5}

Supporting Figure 1. Comparison of the three-dimensional structures of CD22 and MAG proximal Ig domains. Crystal structures of d7 and d5 proximal Ig-like domains of CD22 and MAG, respectively. C1- and C2-type Ig folding contain different β-strand topology of strands D and C´.

Supporting Figure 2

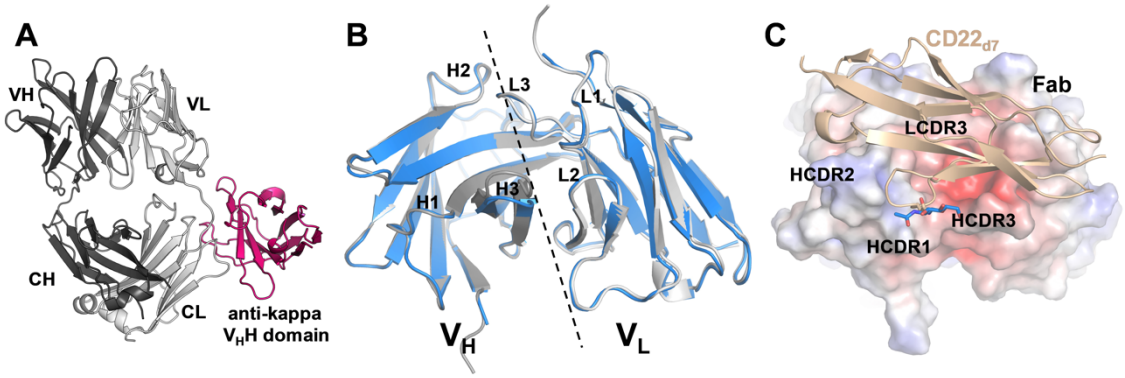

Supporting Figure 2. Variable region of m971 Fab. A) Crystal structure of m971 Fab (grey) in complex with the anti-kappa V_HH domain (magenta). The anti-kappa V_HH domain interacts with the Fab constant region of the light chain (CL). B) Superposition of the crystal structures of the variable domain of m971 Fab unliganded (in blue) and CD22-bound (grey). Except for the HCDR3 loop, no significant changes are observed in the CDRs, indicating that m971 is largely in a predisposed conformation to bind CD22 d7. C) Electrostatic surface representation of the m971 paratope. The d7 domain of CD22 is shown as wheat secondary structure. The calculation of the surface electrostatics was made with the APBS software (1) and prepared using Pymol (2) and displayed on a scale of -5 kT/e (red) to 5 kT/e (blue).

Supporting Figure 3

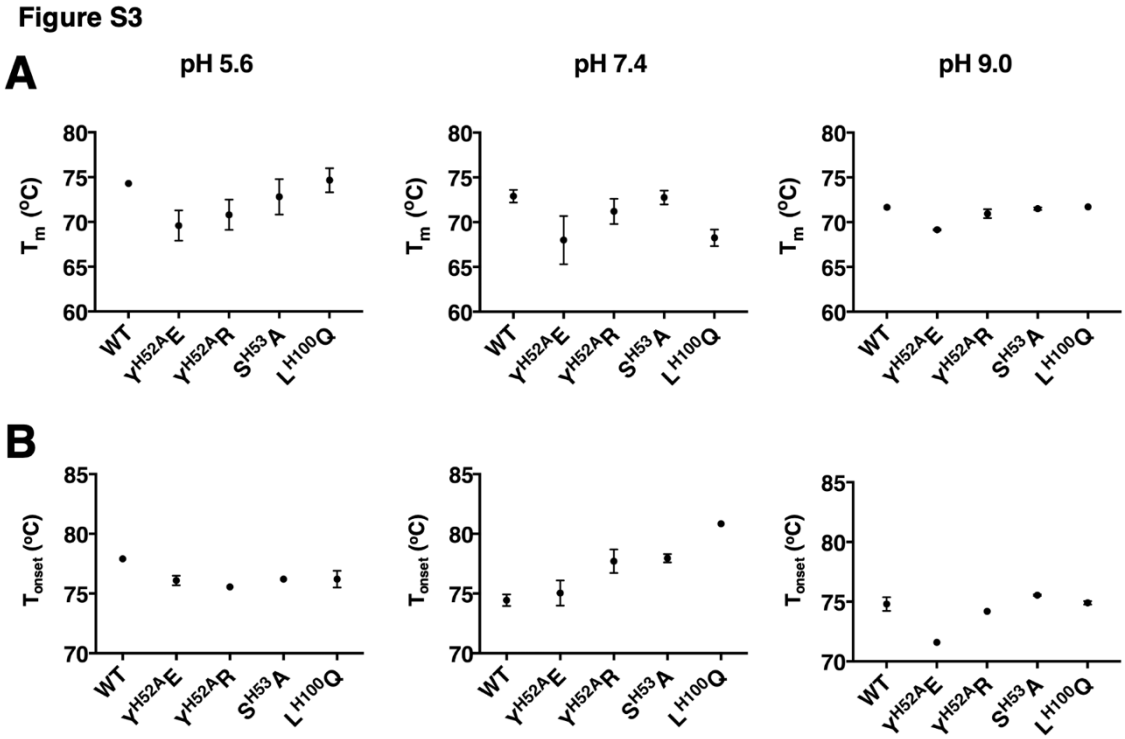

Supporting Figure 3. Thermal stability of WT and mutant m971 Fabs at different pH's. A) Melting temperature (T_m) calculated from intrinsic fluorescence. B) Onset aggregation temperature (T_{onset}) calculated from static light scattering.

Supporting Figure 4

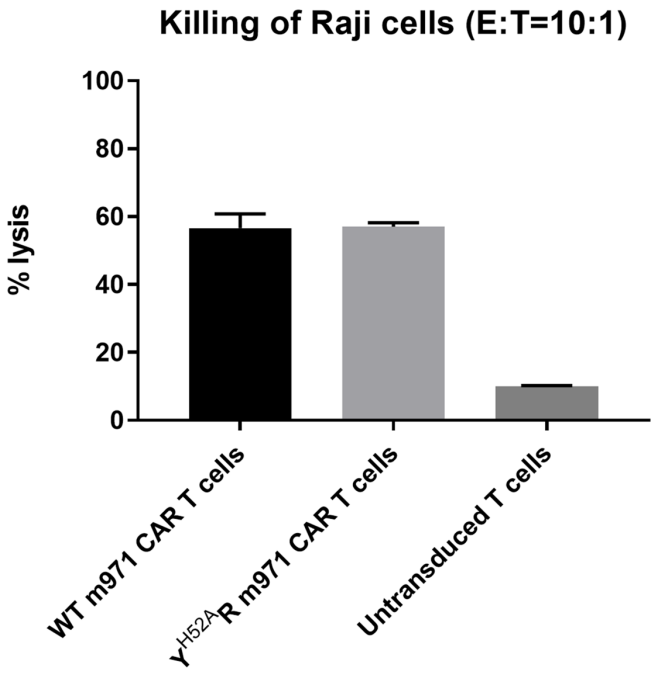

Supporting Figure 4. Lysis of Raji cells by wild type (wt) and $Y^{H52A}R$ mutant m971 CAR-T cells. WT m971 and $Y^{H52A}R$ m971 scFv were incorporated into the 2nd generation CAR with CD28 transmembrane domain and intracellular 4-1BB and CD3 ζ domain, which were expressed on Jurkat T cells surface by lentiviral-mediated transduction. CAR-T cell killing of Raji cells was detected by the Promega CytoTox-Glo™ Cytotoxicity Assay kit. Untransduced T cells were used as a negative control.

Supporting Figure 5

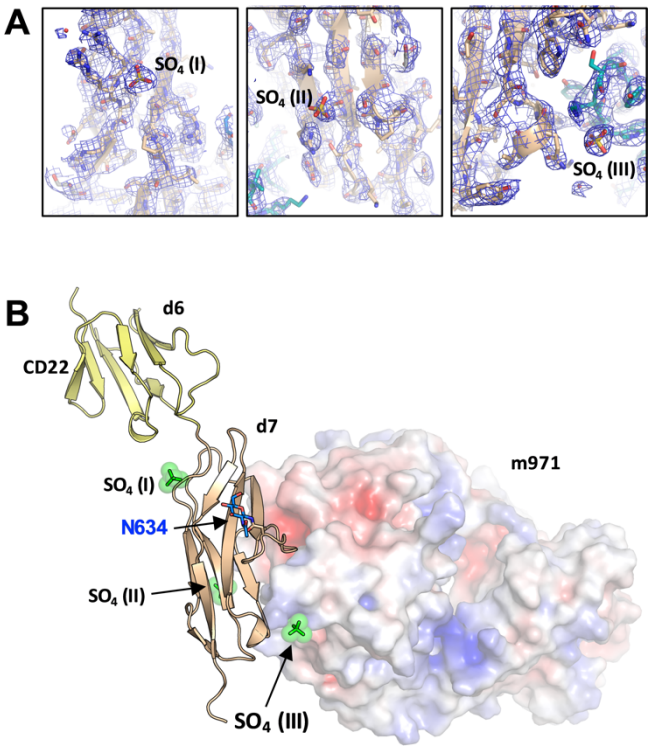

Supporting Figure 5. Sulphate ions in the $CD22_{d6\text{-}d7}$-m971 Fab co-crystal structure. A) Representative electron density showing the sulphate ion sites I (left), II (middle) and III (right) on the surface of CD22 (in wheat color). The electron density was calculated from a composite omit map and contoured at 1σ. B) Crystal structure of $CD22_{d6\text{-}d7}$ in complex with m971 Fab. Electrostatic surface of the m971 Fab is represented. SO_4 III is located at the interface between CD22 and m971. The calculation of the surface electrostatics was made with the APBS software (1) and prepared using Pymol (2) and displayed on a scale of -5 kT/e (red) to 5 kT/e (blue).

Supporting Figure 6

Supporting Figure 6. Sequence alignment of CD22. Amino acid sequence alignment of CD22 from human (hCD22), mouse (mCD22) and rat (rCD22). The red box indicates the putative heparan sulfate binding site, with XBBXBX motif (X, aliphatic residues and B, amino acids R, K or H). Sequence alignment was done using the Clustal Omega software (3).

Supporting Table 1. Residues involved in the m971-CD22 interaction. S= salt bridge; H= hydrogen bond.

Contact type	CD22 residue	BSA (Å^2)
	P623	12
	V624	10
	S625	56
S	H626	71
	Y627	8
H	T628	18
H	D631	16
	W632	35
H	N633	11
H	Q635	62
	S636	28
	L637	32
H	P638	109
H	Y639	70
HS	H640	136
H	S641	52
	Q642	3
	R645	11
	L646	22
HS	E647	65
	P648	43
	K650	15
	Q652	36
H	H653	57
H	Y657	12

	Total	**990**
	m971 HC residue	**BSA (Å^2)**
H	N32	32
	A35	1
H	R50	32
H	Y52	38
	R52b	78
H	S53	64
	K54	65
H	W55	25
H	Y56	99
	N57	37
H	D58	33
	Y59	28
HS	K64	30
	T97	20
	G98	12
HS	D99	74
	L100	26
HS	D100b	28
	Total	**722**
	m971 LC residue	**BSA (Å^2)**
	W30	71
H	Y32	60
	S91	11
H	Y92	78
	S93	15

	I94	41
	Total	**276**

References

1. Unni, S., Huang, Y., Hanson, R. M., Tobias, M., Krishnan, S., Li, W. W., Nielsen, J. E., and Baker, N. A. (2011) Web servers and services for electrostatics calculations with APBS and PDB2PQR. *J. Comput. Chem.* 10.1002/jcc.21720
2. Schrödinger, L. (2015) The PyMol Molecular Graphics System, Versión 1.8. *Thomas Hold.* 10.1007/s13398-014-0173-7.2
3. Sievers, F., and Higgins, D. G. (2014) Clustal omega, accurate alignment of very large numbers of sequences. *Methods Mol. Biol.* 10.1007/978-1-62703-646-7_6